

Plasma- Spray Coating

by. Robert B. Heimann

Copyright© VCH Verlagsgesellschaft mbH. 1996

Appendix A: Dimensionless Groups

Dimensional analysis is a key step in modeling processes [1, 2]. There are usually fewer dimensionless groups than there are physical quantities (Buckingham's rule) [3]. When the model is evaluated or displayed, the dimensionless groups are the correct axes to choose (see, for example Fig. 4-18). It should be emphasized that dimensionless groups should always be used for exponential, logarithmic, or power law arguments since failure to do so may lead to pseudo-constants without physical significance [3].

Because of their ability to simplify complex modeling problems, dimensionless groups are frequently used in chemical engineering to solve complex equations of heat and mass transfer. In particular, equations of heat, mass and impulse transfer ubiquitously occurring in the description of plasma spray processes and numerical solutions of modeling approaches can be deduced from existing solutions of geometrically similar systems [4]. The term 'geometric similarity' refers to the interchangeability of streamlines and boundaries of systems of widely varying dimensional extentions by linear scaling laws. Motion of fluids such as a plasma gas are dynamically similar when the solutions of the related dimensionless transfer equations are identical. For example, the simplified Navier–Stokes equation

$$\rho(\delta v/\delta t) = \rho(v \cdot \nabla)v - \nabla p + \eta\nabla^2v + f, \quad (\text{A-1})$$

where v = mass average velocity (barycentric velocity), p = plasma gas pressure, and η = plasma gas viscosity, can be transformed to its dimensionless version by using the free-stream plasma velocity V , a characteristic length L and a typical pressure p_0 to normalize $v(x, y, z)$ and p by setting

velocity $W = v/V$,

length $X = x/L$, $Y = y/L$, $Z = z/L$, and (A-2)

pressure $P = p/p_0$.

Substituting the dimensionless ratios into Eq. (A-1) yields

$$\rho(V^2/L)(W \cdot \text{grad})W = -(p_0/L) \text{grad}(P) + (\eta V/L^2)\nabla^2W \quad (\text{A-3})$$

or $(W \cdot \text{grad})W = -(p_0/\rho V^2) \text{grad}(P) + \text{Re}^{-1}(\nabla^2W), \quad (\text{A-3a})$

with $\text{Re} = VL/\eta$.

It should be noted that the second term on the right hand side of Eq. (A-3a) contains all the parameters that govern the fluid dynamics of a plasma jet. Dynamic similarity is assured if for two geometrically similar systems A and B, $\text{Re}(A) = \text{Re}(B)$. The similarity principle was discovered by Reynolds and has overriding importance for any modeling approach in fluid dynamics [5].

The most important dimensionless groups used in modeling of plasma heat and mass transfer equations can be conveniently divided into groups describing momentum-, heat-, and mass transfer, and materials constants.

Momentum transfer

Reynolds number	$\text{Re} = VL/v$ (inertia force/viscous force)
Euler number	$\text{Eu} = \Delta p / \rho V^2$ (fluid friction)
Grashof number	$\text{Gr} = L^3 g \gamma \Delta T / v^2$ (bouyancy force/viscous force)

Heat transfer

Fourier number	$\text{Fo} = \kappa \Delta T / L^2$ (heat transfer by diffusion)
Péclet number	$\text{Pe} = VL/\kappa = \text{Re} \times \text{Pr}$ (bulk heat transfer/conductive heat transfer)
Rayleigh number	$\text{Ra} = L^3 g \gamma \Delta T / v \kappa = \text{Gr} \times \text{Pr}$ (free convection)
Nusselt number	$\text{Nu} = hL/k = \text{Re} \times \text{St}$ (total heat transfer/conductive heat transfer)
Stefan number	$\text{St} = \sigma LT^3 / k$ (heat transfer by radiation)

Mass transfer

Fourier number	$\text{Fo}^* = D \Delta T / L^2 = \text{Fo} / \text{Le}$ (unsteady state mass transfer)
Péclet number	$\text{Pe}^* = VL/D = \text{Re} \times \text{Sc}$ (bulk mass transfer/diffusive mass transfer)
Grashof number	$\text{Gr}^* = L^3 g \beta' \Delta x / v^2$ (mass transfer at free convection)
Nusselt number	$\text{Nu}^* = kL / \rho D = \text{Sh}$

Materials constants

Prandtl number	$\text{Pr} = v/\kappa = \text{Pe}/\text{Re}$
Schmidt number	$\text{Sc} = v/D = \text{Pe}^*/\text{Re}$
Lewis number	$\text{Le} = \kappa/D = \text{Sc}/\text{Pr}$

References

- [1] P. Bridgeman, *Dimensional Analysis*, 2nd edn., York University Press, New Haven, CT, USA.
- [2] E. Isaacson, M. Isaacson, *Dimensional Models in Engineering and Physics*, Wiley, NY, USA, 1975.
- [3] M. F. Ashby, *Mater. Sci. Technol.*, **1992**, 8, 102.
- [4] F. Rosenberger, *Fundamentals of Crystal Growth I*, Springer, Berlin, 1979, p. 267f.
- [5] D. F. Boucher, G. E. Alves, *Chem. Eng. Progr.* **1959**, 55, 55.

Plasma- Spray Coating

by. Robert B. Heimann

Copyright© VCH Verlagsgesellschaft mbH. 1996

Appendix B: Calculation of Temperature Profiles of Coatings

The following treatment has been adapted from the work by Houben [1]. It provides the calculations required to arrive at the temperature profiles through Mo and AISI-316 coatings, respectively deposited onto a low carbon steel substrate as shown in Fig. 5-12. The calculations are based on the Neumann-Schwartz equation [2].

B.1 Heat Conduction Equations

For the three regions identified in the coordinate system of Fig. 5-10 the three heat conduction (Fourier) equations can be expressed by

$$\partial^2\Theta_0/\partial x^2 - (1/a_0)\partial\Theta_0/\partial t = 0 \quad \text{for } x \leq 0 \text{ (solid substrate)} \quad (\text{B-1a})$$

$$\partial^2\Theta_1/\partial x^2 - (1/a_1)\partial\Theta_1/\partial t = 0 \quad \text{for } 0 \leq x \leq X(t) \text{ (solid deposit)} \quad (\text{B-1b})$$

$$\partial^2\Theta_2/\partial x^2 - (1/a_2)\partial\Theta_2/\partial t = 0 \quad \text{for } x \geq X(t) \text{ (liquid deposit)}, \quad (\text{B-1c})$$

where Θ = temperature and a = thermal diffusivity.

The boundary conditions are $\Theta_0 = T_{s0}$ (20°C) as $x \rightarrow -\infty$,

$$\Theta_0 = \Theta_1 \quad \text{as } x = 0.$$

$$\Theta_1 = \Theta_2 \quad \text{as } x = X(t)$$

For thermal equilibrium conditions at the interfaces it follows that

$$k_0(\partial\Theta_0/\partial x) = k_1(\partial\Theta_1/\partial x) \quad \text{as } x = 0 \quad (\text{B-3})$$

$$k_1(\partial\Theta_1/\partial x) - k_2(\partial\Theta_2/\partial x) = L\rho(dX/dt) \quad \text{as } x = X(t), \quad (\text{B-4})$$

where L = latent heat of melting.

For the special case indicated in Fig. 5-10 ($\Theta_2 = T_3 = T_m$ for $x \geq 0$) the Eq. (B-4) simplifies to

$$k_1(\partial\Theta_1/\partial x) = L\rho(dX/dt) \quad \text{as } x = X(t). \quad (\text{B-4a})$$

B.2 Solutions of the Equations

B.2.1 Substrate Temperature Profile

$$\text{Assumption: } \Theta_0 = T_{s0} + \alpha[1 + \operatorname{erf}(x/(4a_0 t)^{1/2})]. \quad (\text{B-5})$$

The quantity α is the so-called contact conductivity at the interface substrate/solid deposit ($x = 0$) and is defined as $\alpha = (k_1 \rho_1 c_1)^{1/2}$, where k = thermal conductivity, ρ = density, and c = specific molar heat. It should be emphasized that the solution shown in Eq. (B-5) satisfies both Eq. (B-1a) and, because of $\Theta_0 \rightarrow T_{s0}$ as $x \rightarrow -\infty$, the first boundary condition. The error function erf is as usually defined as $\operatorname{erf} z = \int(2/\pi^{1/2}) \exp(-z^2) dz$.

B.2.2 Deposit Temperature Profile

$$\text{Assumption: } \Theta_1 = T_{s0} + \beta + \gamma \operatorname{erf}(x/(4a_1 t)^{1/2}). \quad (\text{B-6})$$

The quantity β is the contact conductivity at the interface solid/liquid deposit ($x = X(t)$), and γ the ‘contact’ diffusivity at the free interface receiving a constant stream of molten particles. Eq. (B-6) satisfies Eq. (B-1b), and also satisfies the second boundary condition if $\beta = \alpha$ ($\Theta_0 = \Theta_1$ as $x = 0$). Then Eq. (B-6) can be rewritten as

$$\Theta_1 = T_{s0} + \alpha + \gamma \operatorname{erf}(x/(4a_1 t)^{1/2}). \quad (\text{B-6a})$$

To establish the required connection between α and γ the Eqs. (B-5) and (B-6) will be differentiated to yield

$$\begin{aligned} \partial\Theta_0/\partial x &= \alpha[[\partial/\partial x] \operatorname{erf}(x/(4a_0 t)^{1/2})] \\ &= \alpha(2/\pi^{1/2}) \exp(-x^2/4a_0 t)(1/(4a_0 t)^{1/2}) \\ &= [\alpha/(\pi a_0 t)^{1/2}] \exp(-x^2/4a_0 t). \end{aligned} \quad (\text{B-7})$$

For $x = 0$ it follows that

$$(\partial\Theta_0/\partial x)_{x=0} = \alpha/(\pi a_0 t)^{1/2}. \quad (\text{B-7a})$$

Analogously one obtains

$$(\partial\Theta_1/\partial x)_{x=0} = \gamma/(\pi a_1 t)^{1/2}. \quad (\text{B-7b})$$

Substituting Eqs. (B-7a) and (B-7b) into (B-3) yields

$$k_0(\alpha/(\pi a_0 t)^{1/2}) = k_1(\gamma/(\pi a_1 t)^{1/2}).$$

With $\alpha/\gamma = B$, and $a = k/\rho c$ one obtains

$$B = (k_1 \rho_1 c_1)^{1/2} / (k_0 \rho_0 c_0)^{1/2}. \quad (\text{B-8})$$

With Eq. (B-8), Eq. (B-6a) can be expressed as

$$\begin{aligned} \Theta_1 &= T_{s0} + \gamma[(\alpha/\gamma) + \operatorname{erf}(x/(4a_1 t)^{1/2})] \\ &= T_{s0} + \gamma[B + \operatorname{erf}(x/(4a_1 t)^{1/2})]. \end{aligned} \quad (\text{B-9})$$

For $\Theta_1 = \Theta_2 = T_m$ (as $x \geq X(t)$) we obtain the explicit solution of the heat transfer equation at the interface liquid/solid deposit as

$$T_m - T_{s0} = \gamma[B + \operatorname{erf}(x/(4a_1 t)^{1/2})]. \quad (\text{B-10})$$

With the assumption

$$X = p(4a_1 t)^{1/2} \quad \text{or} \quad t = X^2/4p^2 a_1 \quad (\text{B-10a})$$

(solution of the first-order differential equation of heat transfer) it follows that

$$dX/dt = p(a_1/t)^{1/2}. \quad (\text{B-11})$$

With Eq. (B-7) for $x = X(t)$, Eq. (B-4a) can further be expressed by

$$k_1(\gamma/(\pi a_1 t)^{1/2}) \exp(-X^2/4a_1 t) = L\rho (dX/dt) \quad (\text{B-12})$$

and with (Eq. B-11) as

$$k_1(\gamma/(\pi a_1 t)^{1/2}) \exp(-X^2/4a_1 t) = L\rho p (a_1/t)^{1/2}. \quad (\text{B-13})$$

From Eqs. (B-10 and 10a) it follows that

$$\gamma = (T_m - T_{s0})/[B + \operatorname{erf}(X/(4a_1 t)^{1/2})] = (T_m - T_{s0})/(B + \operatorname{erf} p). \quad (\text{B-14})$$

Inserting Eqs. (B-14) and (B-10a) into Eq. (B-13) yields

$$(k_1/(\pi a_1 t)^{1/2})[(T_m - T_{s0})/(B + \operatorname{erf} p)] \exp(-X^2/4a_1 t) = L\rho p (a_1/t)^{1/2} \quad (\text{B-15})$$

$$\text{or} \quad (k_1/(\pi a_1 t)^{1/2})[(T_m - T_{s0})/(B + \operatorname{erf} p)] \exp(-p^2) = L\rho p (a_1/t)^{1/2}. \quad (\text{B-15a})$$

If the density of the molten particles equals the density of the solid material ($\rho = \rho_1$), Eq. (B-15a) can be expressed as

$$(k_1/(\pi a_1 t)^{1/2})[(T_m - T_{s0})/(B + \operatorname{erf} p)](1/(a_1/t)^{1/2}) = (L\rho_1 p) \exp(p^2), \quad (\text{B-16})$$

and finally, because $c_1 = k_1/\rho_1 a_1$,

$$(B + \operatorname{erf} p)p \exp(p^2) = c_1(T_m - T_{s0})/L(\pi)^{1/2}. \quad (\text{B-17})$$

Eq. (B-17) can be used to determine the constant p from the energy balance at the solidification front. It can also be taken from a nomogram provided by Kuijpers and Zaai [2]. With this one can also determine the *real temperature profiles*.

B.3 Real Temperature Profiles

From Eq. (B-8) it follows that $\alpha = \gamma B$, and with Eq. (B-14) one obtains

$$\alpha = [B(T_m - T_{s0})]/[B + \operatorname{erf} p]. \quad (\text{B-18})$$

Inserting Eq. (B-18) into Eq. (B-5) yields the *real substrate temperature profile*

$$\Theta_0 = T_{s0} + \{[B(T_m - T_{s0})]/[B + \operatorname{erf} p]\}\{1 + \operatorname{erf}(X/(4a_0 t)^{1/2})\}. \quad (\text{B-19})$$

Likewise, the *real solid deposit temperature profile* becomes

$$\Theta_1 = T_{s0} + \{(T_m - T_{s0})/[B + \operatorname{erf} p]\}\{B + \operatorname{erf}(X/(4a_1 t)^{1/2})\}. \quad (\text{B-20})$$

On rewriting the Eqs. (B-19) and (B-20) yield their final expressions:

$$(\Theta_0 - T_{s0})/(T_m - T_{s0}) = [B/(B + \operatorname{erf} p)][1 + \operatorname{erf}(X/(4a_0 t)^{1/2})] \quad (\text{B-19a})$$

and

$$(\Theta_1 - T_{s0})/(T_m - T_{s0}) = [1/(B + \operatorname{erf} p)][B + \operatorname{erf}(X/(4a_1 t)^{1/2})]. \quad (\text{B-20a})$$

These equations should be compared with the approximate expression obtained for transient heat conduction in solid spheres as shown earlier:

$$(T_m - T_R)/(T_m - T_1) = f(Bi, Fo) = f[\alpha\Theta/r^2] = f[a_1 t/r_0^2] \quad (4-23)$$

References

- [1] J. M. Houben, Relations of the adhesion of plasma sprayed coatings to the process parameters size, velocity and heat content of the spray particles. Ph.D. Thesis, Technical University Eindhoven, The Netherlands, 1988.
- [2] T. W. Kuijpers, J. H. Zaai, *Met. Technol.* 1974, March, 142.

Plasma- Spray Coating

by. Robert B. Heimann

Copyright© VCH Verlagsgesellschaft mbH. 1996

Appendix C: Calculation of Factor Effects for a Fractional Factorial Design 2^{8-4}

In this example, calculations will be shown for estimating factor effects for the dependence of the thickness of a plasma-sprayed 88WC12Co coating on the eight selected plasma parameters and their ranges (Table C-1). To avoid bias (systematic) errors the 16 experimental runs to be performed were randomized. This randomized fractional two-level factorial design is shown in Table C-2.

The 2^{8-4} design chosen is a 1/16 replicate of a full 2^8 factorial of resolution IV that has the power to estimate the eight main factor effects X_i clear of each other, and clear of composite two-factor interactions E_i ¹. The effects of higher-order interactions can usually be safely neglected. Composite effects of the sum of four two-factor interactions, however, can be estimated from the unassigned factors. If only weak or no interactions exist, the effects of unassigned factors can be used to estimate the experimental (statistical) error, i.e. the minimum significant factor effect. The arrangement of the coded parameter levels in the design matrix (Table C-3) follows Yates' standard order.

Tables C-3 and C-4 show the numerical evaluation of the results for the main factor effects X_i and the composite two-factor interactions E_i . First the sum $\sum(+)$ of all responses Y (thickness of coating) on the '+' level is calculated. Then the $\sum(-)$ of all responses Y on the '-' level is calculated. The factor effect is the difference Δ of the two sums, divided by the number of '+' (or '-') signs in each column. The coefficients, C , of the parameters in the polynomial response equation are obtained by dividing

¹ The confounding pattern of the composite two-factor interactions E_i is as follows:

$$\begin{aligned} E_1 &= X_1X_2 + X_3X_7 + X_4X_8 + X_5X_6 = \mathbf{12 + 37 + 48 + 56} \\ E_2 &= \mathbf{13 + 27 + 58 + 36} \\ E_3 &= \mathbf{14 + 28 + 36 + 57} \\ E_4 &= \mathbf{15 + 38 + 26 + 47} \\ E_5 &= \mathbf{16 + 78 + 34 + 25} \\ E_6 &= \mathbf{17 + 23 + 68 + 45} \\ E_7 &= \mathbf{18 + 24 + 35 + 67} \end{aligned}$$

Table C-1. Plasma spray parameter and their ranges used to estimate the factor effects on coating thickness and microhardness.

	Plasma Spray Parameter	Ranges	
X_1	Plasma arc current	700–900 A	
X_2	Argon gas pressure	0.34–1.36 MPa	
X_3	Helium gas pressure	0.34–1.36 MPa	
X_4	Powder gas pressure	0.34–0.68 MPa	
X_5	Powder feed rate	0.50–2 (scale value)	
X_6	Powder grain size	(−45 + 5)–(−75 + 45) μm	
X_7	Number of passes	1st set 2nd set	5–15 20–30
X_8	Spray distance	20–45 cm	

Table C-2. Fractional two-level factorial design in variables 1 to 8 and the response Y (coating thickness) and its standard deviation.

Run #	X_1	X_2	X_3	X_4	X_5	X_6	X_7	X_8	Resp. Y (μm)	σ (μm)
1	700	0.34	0.34	0.68	2	Coarse	20	45	118	79
2	900	0.34	0.34	0.34	0.5	Coarse	30	45	16	8
3	700	1.36	0.34	0.34	2	Fine	30	45	203	111
4	900	1.36	0.34	0.68	0.5	Fine	20	45	57	25
5	700	0.34	1.36	0.68	0.5	Fine	30	45	82	35
6	900	0.34	1.36	0.34	2	Fine	20	45	138	87
7	700	1.36	1.36	0.34	0.5	Coarse	20	45	30	12
8	900	1.36	1.36	0.68	2	Coarse	30	45	82	44
9	900	1.36	1.36	0.34	0.5	Fine	30	25	7	4
10	700	1.36	1.36	0.68	2	Fine	20	25	108	104
11	900	0.34	1.36	0.68	0.5	Coarse	20	25	65	30
12	700	0.34	1.36	0.34	2	Coarse	30	25	16	10
13	900	1.36	0.34	0.34	2	Corase	20	25	26	21
14	700	1.36	0.34	0.68	0.5	Coarse	30	25	9	12
15	900	0.34	0.34	0.68	2	Fine	30	25	30	13
16	700	0.34	0.34	0.34	0.5	Fine	20	25	22	19

the factor effect by two. Factor significance is checked against the minimum factor significance, $\{\min\} = \sigma_{FE} t_{\alpha,df}$ where $\sigma_{FE} = [(1/n) \sum E_i^2]^{1/2}$ with $t_{\alpha,df}$ = Student's t -value for a confidence level α of a double-sided significance test and df = degrees of freedom. All absolute factor effects larger than $\{\min\}$ are considered to be statistically significant.

Note that the second half of the main effect design matrix (Table C-3) is the mirror image of the first half, and that the two halves of the composite two-factor inter-

Table C-3. Computing of main factor effects according to Yates' algorithm.

Run	Main	X_1	X_2	X_3	X_4	X_5	X_6	X_7	X_8	Y
1	+	-	-	-	+	+	+	-	+	118
2	+	+	-	-	-	-	+	+	+	16
3	+	-	+	-	-	+	-	+	+	203
4	+	+	+	-	+	-	-	-	+	57
5	+	-	-	+	+	-	-	+	+	82
6	+	+	-	+	-	+	-	-	+	138
7	+	-	+	+	-	-	+	-	+	30
8	+	+	+	+	+	+	+	+	+	82
9	+	+	+	+	-	-	-	+	-	7
10	+	-	+	+	+	+	-	-	-	108
11	+	+	-	+	+	-	+	-	-	65
12	+	-	-	+	-	+	+	+	-	16
13	+	+	+	-	-	+	+	-	-	26
14	+	-	+	-	+	-	+	+	-	9
15	+	+	-	-	+	+	-	+	-	30
16	+	-	-	-	-	-	-	-	-	22
$\sum(+)$	1009	421	522	528	551	721	362	445	726	
$\sum(-)$	0	588	487	481	458	288	647	564	283	
$\sum\sum$	1009	1009	1009	1009	1009	1009	1009	1009	1009	
Δ	1009	-167	35	47	93	433	-285	-119	443	
Effect	63	-21	4	6	12	54	-36	-15	55	
c	b_0	-11	2	3	6	27	-18	-8	28	

action design matrix are identical (Table C-4). From Table C-4 the minimum factor effect can be calculated as follows:

$$\sigma_{FE} = [(1/n) \sum E^2]^{1/2} = (3592/7)^{1/2} = 22.6 \quad (C-1a)$$

$$\{\min\} = \sigma_{FE} t_{\alpha=0.90; df=7} = 22.6 \times 1.895 = 43. \quad (C-1b)$$

Thus, all factor effects whose absolute values are larger than 43 are significant at a confidence level of 90%. From Table C-3 it follows that X_5 (powder feed rate) and X_8 (stand-off distance) are the only significant main factor effects. This holds true even when the confidence level is increased to 95%. There are no significant composite two-factor interactions (Table C-4). Both main factor effects have positive signs, i.e. the coating thickness increases with increasing powder feed rate and increasing spray distance. Hence the response polynomial can be roughly expressed by the equation

$$d[\mu\text{m}] = 63 + 27X_5 + 28X_8. \quad (C-2)$$

Table C-4. Computing of composite two-factor interactions.

Run	E_1	E_2	E_3	E_4	E_5	E_6	E_7	Y
1	+	+	-	-	-	+	-	118
2	-	-	-	-	+	+	+	16
3	-	+	+	-	+	-	-	203
4	+	-	+	-	-	-	+	57
5	+	-	-	+	+	-	-	82
6	-	+	-	+	-	-	+	138
7	-	-	+	+	-	+	-	30
8	+	+	+	+	+	+	+	82
9	+	+	-	-	-	+	-	7
10	-	-	-	-	+	+	+	108
11	-	+	+	-	+	-	-	65
12	+	-	+	-	-	-	+	16
13	+	-	-	+	+	-	-	26
14	-	+	-	+	-	-	+	9
15	-	-	+	+	-	+	-	30
16	+	+	+	+	+	+	+	22
$\sum(+)$	410	644	505	419	604	413	448	
$\sum(-)$	599	365	504	590	405	596	561	
$\sum\sum$	1009	1009	1009	1009	1009	1009	1009	
Δ	-189	279	1	-171	199	-183	-113	
Effect	-24	35	0	-21	25	-23	-14	
c	-12	18	0	-11	13	-12	-7	

Plasma-Spray Coating

by Robert B. Heimann

Copyright © VCH Verlagsgesellschaft mbH. 1996

Index

- Abbot curve 158f
Abel's inversion 79
ablation of particles 104f
abrasion
– gouging abrasion 268
acoustic emission (AE) 267
adhesion number 269
adhesive 229, 249ff
adiabatic diesel engine 15
advanced structural ceramics 3, 4
aerospace industry 2, 8, 209
application technology mapping 311
Archimedes' method 166
Archimedes' technique 247
automated image analysis 165
automotive industry 2, 8
– ceramic engine parts 5
- Basset–Boussinesq–Oseen equation 101, 103
Basset history term 101, 104
bearings 15
behavior surface 125f
bench-scale test 277
Bennett equation 57
Bernoulli method 150
Bernoulli's theorem 82
Biot modulus 217
Biot number 109, 112
bipolar plate 235
blades 15
boiler tubes 8, 15, 196, 274
boilers 196
Boltzmann number 125f
Bouguer number 126
Bragg angle 171
Bragg equation 171
Buckingham's rule 317
- Burner Rig test 220, 279ff
calender rolls 15
cathode fall 45
cathode layer 45
cavitation erosion 183, 202, 220, 268
centrifugal pumps 183, 202
ceramic properties
– chemical stability 14
– coefficient of thermal expansion 14
– fracture toughness 14
– hardness 14
– heat conductivity 14
– high porosity 14
– thermal stability 14
characteristic temperature 109
Charpy impact test 189
chemical bonding type 286
chemical corrosion 183, 191, 202, 206,
279
chemical processing 2
choke nozzles 183f, 187
Clausius–Clapeyron's equation 147
Cline–Anthony model 220
coating application 15
– abradable coating 15
– bioceramic coating 2, 8, 14, 164, 224ff,
311f
– biomedical coating 15
– chemical barrier coating 8
– cocking 15
– corrosion 15
– corrosion-resistant coatings 181ff
– diamond coating 14
– electrocatalytic coating 14
– electromagnetic interference 15
– erosion protection 15

- friction properties 15
- functional ceramic coating 313
- functional coatings 181, 199
- functional plasma-sprayed coatings 232
- high temperature-coating 10, 11
- hot gas erosion 15
- HT-superconducting (HTSC) coatings 232f
- hypervelocity oxyfuel gun (HVOF) 10
- superconducting coating 14
- thermal and chemical barrier coatings 209ff
- thermal barrier bioceramic coatings 100
- thermal barrier coating (TBC) 8, 10, 97, 131, 132, 164, 177, 178, 201, 248, 259, 277, 287, 311ff
- thermal barrier top coating 207
- thick thermal barrier coating 297
- tribological coating 183, 210
- vacuum plasma spraying/low pressure plasma spraying 10
- wear application 15
- wear barrier coating 8, 311f
- wear control 15
- wear-resistant coatings 161, 164, 181ff, 208
- yttria–partially stabilized zirconia coatings 209ff
- coating composition 23
- AISI-316 stainless steel 152ff
- AlN 288
- Al–Si/polyester 296
- Al₂O₃ 112, 131, 181, 199, 253, 285ff
- Al₂O₃/TiO₂ 259, 297
- Al₂O₃/2.5% TiO₂ 172
- 97Al₂O₃3TiO₂ 294
- alumina 8, 21, 63, 70, 77, 80, 83, 91, 97, 101, 102, 109–111, 119, 128–130, 132–134, 142, 148, 149, 177, 201, 202ff, 211, 218, 223, 268
- alumina–titania 210, 268, 305ff
- B₄C 112, 181
- Bi–Sr–Ca–Cu–oxide 232
- C₃P³ 224
- CaO–SiO₂–ZrO₂ 223
- calcium phosphate 224
- η -carbide 168, 184ff, 201, 300, 302
- carbides 93, 97, 168, 181, 199
- cemented carbides 182, 201
- ceramic coating 2, 3, 6, 8, 14, 15
- ceramic membranes 15
- chemical coatings 6
- chromium 8, 164, 167, 201, 204ff, 258ff
- chromium carbide 94, 168, 196ff
- chromium carbide–nickel–chromium (Cr₃C₂–NiCr) composites 21, 268
- chromium oxide 235, 268
- CoCrAlY 131, 211
- CoCrNiW 199
- cobalt 10, 97
- composite coating 14
- composite materials 100
- copper 122–124
- CrB₂ 200
- 94Cr5Fe1Y₂O₃ 235
- Cr₂AlC 183
- Cr₂O₃ 181, 285
- Cr₃C₂ 181, 182
- Cr₃C₂/NiCr 297
- Cr₃C₂–25% NiCr 264f
- 80Cr₃C₂/20(NiCrMo) 275
- 62Cr₃C₂5W₂C₅TiC4Ni3Mo1Cr 200
- Cr₃O₄ 205
- Cr₇C₃ 182, 196, 199
- Cr₂₃C₆ 182
- Cr_xC_y 191
- CT 227
- CT₂ 227
- density 97
- diamond 181, 207ff
- diamond coating 2, 14, 311ff
- diamond films 7
- diamond-like coating 15
- dicalcium silicate 223
- FeCrAlY 199
- 85Fe15Si 140, 294, 303
- FeTi 200f
- ferrosilicon 303ff
- fluorapatite 226
- gallium arsenide 7
- glass-based coating 6
- graded coating 23, 132
- graded metal–ceramic coating 178
- H-phases 183
- hafnium nitride 174
- Hastelloy 205
- HfC 182
- hydroxyapatite 15, 155, 156, 224ff
- Inconel 205
- indium phosphide 7
- indium tin oxide 6
- iron 10, 97
- kaolin 131
- LaCoO₃ 233, 236
- LaCrO₃ 235

- LaMnO₃ 233
- LaSrMnO₃ 233
- (La,Sr)(Ni,Co)O₃ 236
- MCrAlY 218
- M₆C 184
- M₁₂C₄ 184
- metal–ceramic composites 21
- metal coating 14, 15, 93, 166
- metal composites 21
- metallic coatings 205ff
- MoC_{1-x} 182
- MoO₂ 205
- Mo₂C 181, 182, 285
- molybdenum 91, 93, 112, 138, 142, 151ff, 168, 181, 205, 208, 253
- Nb 205
- NbC 181, 182
- Nb/Hf 206
- 89Nb10Hf1Ti 206
- Ni 211, 233
- Ni alloy–Al₂O₃ 235f
- Ni alloy–CSZ 235
- NiAl 100, 207
- NiAl–ZrO₂ 233
- Ni–Al₂O₃ 233
- NiCrAlY 181, 205, 207, 214, 218
- NiCr 254, 293
- NiCrAl/bentonite 296
- NiCrAlMo 259
- NiCrAlMo/ Al₂O₃–TiO₂ 262
- NiCrAlY 62, 214, 223
- NiCrAl/Y–PSZ 288
- Ni–Cr–10B–Si 183
- 73Ni15Cr4Si4Fe3B1C 186ff
- Ni₃Al 207
- nickel 10, 97, 112
- nickel aluminide 165, 167, 172, 198, 218
- nickel-base alloy 297
- nitrides 168
- nonferrous metals 10, 93, 94
- organic paint coating 6
- oxide coating 201ff
- oxides 93
- oxyhydroxyapatite 226
- partially stabilized zirconia (PSZ) 200
- perovskite 236
- polymer coating 8
- polymers 165
- Resistic CM 192
- Resistic CS-40 192
- Resistic HT-6A 192
- SiAlON 276, 285
- SiC 276, 288
- SiO₂ 112
- Si₃N₄ 276, 285
- silica 218
- silicon nitride 83, 311f
- spinel 236
- stabilized zirconia 15, 177, 201
- stainless steel 254
- steel 93, 94, 112
- stellite 308
- Stellite 6 192
- superalloys 15, 205
- superconducting coating 2, 15, 311
- Ta 112, 181, 205, 206
- TaC 112, 181, 182, 285
- TAFALOY 45CT 206
- 90Ta10W 206
- tetracalcium phosphate 226ff
- Ti 181, 205, 294
- 92.5Ti5Al2.5Fe 206
- TiB₂ 200f, 285
- TiC 112, 168, 181, 182, 285ff
- (Ti,Mo)C/NiCo 174, 271, 293, 296
- TiN 112, 285ff
- TiO₂ 181
- Ti₂AlC 183
- tin oxide 6
- titanium 8, 168, 194, 309
- titanium carbide 8, 191ff, 313
- titanium nitride 174, 313
- tricalcium phosphate 15
- tungsten 94, 131, 168, 208, 257, 298
- tungsten carbide 267
- tungsten carbide/cobalt coatings 183f, 299ff
- tungsten carbide–cobalt (WC–Co) composites 21
- UO₂ 112
- VN 288
- VC 182
- W 112, 181, 205
- WC 181, 182, 285ff
- 88WC12Co 186ff, 293, 294, 298, 323
- WC/Co coating 168, 268, 297
- WC/Co(Ni) 169
- W₂C 182
- Y–Ba–Cu–oxide 232
- yttria 211
- yttrium 99
- zirconia 8, 21, 83, 97, 99, 117, 207, 233,

- 259, 267
- zirconia–NiCrAlY 276f
- ZrC 112, 182
- ZrO₂ 112
- t-ZrO₂/α-Al₂O₃ 174
- ZrO₂·Y₂O₃ 131
- ZrO₂–8wt% Y₂O₃–NiCrAlY 249
- coating diagnostics 153
 - adhesion of coatings 167f
 - adhesion strength 313
 - Almen-type test 174ff
 - area law of mixture 264f
 - back wall echo 258
 - blind hole test 170, 177
 - chemical adhesion 167
 - dry sand-rubber wheel abrasion test 271, 273
 - four-point bending test 267
 - interface echo 259, 261
 - macrobonding 167
 - macroroughness 157, 167
 - macroscopic stresses 169
 - measurement of porosity 165
 - mechanical anchorage 167
 - mesoscopic stresses 169
 - microbonding 167
 - microroughness 157
 - microscopic stresses 169
 - microstructure 153, 155, 161, 163, 165
 - particle velocity 164
 - peel test 255f
 - physical adhesion 167
 - pin-hole test 254
 - residual stresses 169ff, 174ff
 - roughness 159, 161
 - a-scan diagram 258
 - c-scan diagram 258ff
 - scratch energy density 271
 - scratch test 255ff, 263
 - shear test 254f
 - sin²π-technique 171
 - surface roughness 155ff, 160, 161, 167, 174, 199, 269, 296
 - tensile test 248ff, 259
 - thermal wave scanning 259f
 - three-point bend test 267
 - (Ti,Mo)C–NiCo 255
 - ultrasonic signal 255ff
 - ultrasonic test 257ff
 - wipe test 156
- coating properties 10
 - abrasion resistance 187, 203, 271
 - adhesion 142, 153, 161, 285
 - adhesion strength 1, 97, 100, 148, 161, 202, 226, 248ff, 261
 - adhesive bonding 137
 - bending strength 211
 - bond strength 246, 248ff
 - chemical changes 168
 - chemical properties 247, 275
 - coating 142
 - coating adhesion 229
 - coating cohesion 169
 - coating density 19
 - coating porosity 137, 217, 229
 - cohesion 91, 142, 148
 - cohesive bonding 137
 - cohesive strength 248ff, 262, 300
 - composite hardness 263f
 - corrosion resistance 203, 212, 214
 - density 97
 - electronic conductivity 6
 - erosion resistance 199, 212, 223, 296f
 - fatigue 97, 196, 209
 - ferroic coating 311
 - fractal approach 1
 - fracture toughness 4, 100, 161, 202, 205, 211, 218, 224, 266f, 271, 285
 - frictional properties 158, 161, 183, 191
 - functional properties 23
 - hardness 100, 161, 296f
 - hot corrosion resistance 223
 - Knoop indentation test 262
 - low-cycle 277
 - low cycle fatigue 206
 - macrohardness 97
 - macrohardness test 261ff
 - mechanical properties 23, 247f, 277
 - mechanical strength 4
 - microhardness 187, 191, 202, 205, 212, 267, 296f, 300, 302, 304
 - microhardness test 261ff
 - microporosity 148
 - microstructure 1, 23, 203, 207, 229, 263, 267, 268, 277
 - oxidation resistance 187, 212, 214
 - piezoelectric coating 311
 - piezo- or ferroelectric properties 6
 - porosity 97, 99, 157, 161, 164, 212, 263, 296f, 297, 302
 - residual stress 1, 201, 202, 213ff, 229,

- 263, 267, 268
- Rockwell hardness 184, 186
- Rockwell hardness test 262
- superconducting coating 311f
- tensile strengths 91, 262, 296f
- thermal fatigue 277
- tribological properties 247, 268
- Vickers hardness 263
- Vickers indentation test 262
- wear resistance 97, 192, 196, 202, 203, 223
- coating techniques 3ff
 - chemical vapor deposition (CVD) 2, 7, 207, 285
 - diffusion coating 184, 196ff, 206
 - electron-beam deposition 23
 - electron-beam physical vapor deposition 206
 - evaporation 7
 - ion implantation 7
 - laser ablation 7, 207
 - magnetron sputtering 7
 - physical vapor deposition (PVD) 2, 7, 285, 287
 - plasma-assisted vapor deposition 35, 207
 - RF sputtering 225
 - sol-gel technique 2, 6, 94, 165
 - sputtering methods 7
- color temperature 80
- combustion gas
 - acetylene 17, 21, 194, 208
 - butane 17
 - chemical energy 17
 - ethane 194
 - internal enthalpy 48
 - methane 194, 207
 - propane 17, 21, 194
 - propylene 196
- combustor can 15, 275
- component test 277
- concrete bridges 15
- concrete floors 15
- conservation 48
- conservation equations 55, 121f
 - of continuity 121
 - of energy 48, 121, 144, 145
 - of mass 48, 144, 145
 - of momentum 48, 57, 121, 144, 145
 - species conservation 121
- construction industry 2
- continuous wave photothermal radiometry 261
- control surface 125f
- convection-diffusion equation 117
- Coriolis forces 57
- corrabrasion 204
- Coulter Counter 247
- cracking furnace tubes 15
- critical current density 233
- cross-correlation function (CCF) 88
- crucible test 279ff
- crystal growth kinetics 137
- cutting tools 182, 208, 285, 313
- cytotoxic response 226
- Dean test 279, 281
- decarburization 181ff, 199, 201
- degree of crystallinity 226
- delamination 214, 216, 220
- dense loading conditions 101, 119ff, 124
- dental prostheses 15
- deposition efficiency 19, 21, 77, 94, 97, 100, 139, 297
- deposition rates 23
- deposition time 139
- design of
 - data bases 10
 - equipment 10
 - expert systems 10
 - software 10
 - spray powder 10
- design of coatings 285ff
- design of experiments 243ff
 - Box-Behnken design 290, 294f, 297
 - central composite design 295
 - confounding pattern of two-factor interactions 323
 - factorial design 293f
 - four-dimensional hypercube 300f, 304
 - fractional factorial design 293f, 299ff, 305, 323ff
 - full factorial design 293, 297f
 - limited response surface experiment 290
 - minimum factor significance 291, 300, 324f
 - minimum significant factor effect 323
 - multifactorial analysis 243
 - multifactorial design 303
 - orthogonal blocking 295
 - Plackett-Burman design 289ff, 296, 298
 - power of resolution 294
 - precision ratio 292
 - response surface 299, 303, 304
 - response surface methodology 289f

- rotatability 295
- statistical design of experiments (SDE) 10, 97, 288
- statistical experimental strategy (SES) 244
- statistical multifactorial experimental designs 184
- supersaturated design 290
- Taguchi design 289, 296, 298
- two-level factorial analysis 289
- Wheeler's test 292
- Yates algorithm 293
- Yates order 293
- diamond indenter 263, 272
- diamond penetrator 262
- dielectric breakdown strength 202
- Dietzel equation 170, 178
- dimensionless groups 125, 317f
- Dirac delta function 151
- drag coefficient 103ff, 108, 149
- drag force 69, 101, 104, 149
- dwell time 119
- ease of melting parameter 112, 113
- elastic modulus 288
- electrical conductivity 50, 60
- electrochemical machining 235
- electrode 35, 42, 47, 61, 62, 64, 68–70, 231
 - anode 46, 54, 55, 60, 62, 63, 74, 233, 235
 - cathode 46, 50, 52, 54, 60, 63, 91, 233, 235
 - cold cathode 46
 - contamination 61, 64
 - hot cathode 46
 - electron emission 46, 50–52, 60
 - field emission 46
 - thermal emission 46
 - thermionic emission 41, 50–52
- electron mobility 50, 57
- electron work function 41, 50–52, 60
- electron-gas interactions 27
- electronics industry 2
- Elenbaas–Heller equation 48
- emission coefficient 79
- emission intensity 80
- emissivity 77, 80, 121, 125, 126, 259
- energy economy 126
- energy efficiency 127
- energy transfer process 22, 24, 27ff, 137
- Euler flow equation 57
- Euler number 318
- evaporation constant 119f
- extrusion dies 15
- fast Fourier transformation (FFT) analyzer 88
- Fick's law 150, 167
- finite element 155
- finite element analysis 214, 216
- flame torch 19, 48
 - D-Gun system 17
 - hypervelocity oxyfuel gun (HVOF) 17, 21
 - Jet Kote system 17
 - oxyacetylene torches 17
- flight distance 141
- Fourier analysis 163
- Fourier number 112, 143, 318
- fractals
 - ballistic model 138, 159
 - box counting method 161f
 - characteristic correlation length 160
 - correlation length 163
 - density correlation function 161
 - dilatation symmetry 158
 - fractal dimension 158–161, 163, 167
 - fractal properties 154, 158
 - fracture profile analysis (FPA) 163
 - height difference correlation function 160
 - mass correlation function 163
 - mass fractals 158
 - percolative scaling 161
 - self-affinity 160
 - self-similarity 158
 - slit island analysis (SIA) 163
 - surface fractals 158
- friction coefficient 269
- functional gradient materials 287
- gas turbine 10, 11, 15, 62, 209, 211–213, 275, 279, 287
- gas turbine blades 132
- gas turbine vanes 15
- Gauss' principle 165
- Gerdien arc 63, 69
- Grashof number 125, 318
- grey body radiation 80
- Grey probe 81f
- Hall Flow Funnel 247
- He–Ne laser 130
- heat conduction in solid spheres 111, 322
- heat conduction potential 114ff
- heat diffusion equation 140

- heat flow 139
- heat flux potential 48
- heat flux ratios 118
- heat loss 61
 - convection 61
 - conductive heat losses 221
 - convective heat losses 175
 - radiation 61
 - radiative heat losses 221
- heat sinks 15
- heat transfer 22, 41, 81, 101, 106ff, 119, 137
 - between plasma and particles 132
 - convective energy transfer 122
 - equation of heat transfer 317
 - Fourier's law 149
 - from particles to substrate 149
 - from plasma to particles 38, 50
 - heat flux 61, 64
 - heat transfer catastrophe 122ff
 - heat transfer equation 141, 142, 150, 152
 - heat transfer model 177
 - low loading conditions 106
 - modeling 127
 - radiative energy transfer 122
 - rates 60
 - to substrate 151
- heat transfer coefficient 106, 108, 125
- heat transfer equations 113ff
- hip prostheses 224
- Hooke's law 170
- Hugoniot adiabate 145f
- hydrogen arc 48f, 70
- hydrogen plasma jet 101

- I-U* characteristic 45
- indentation size effect 263, 266
- immersion test 279
- interface parameter 266
- intermission time 137, 140, 141
- internal combustion engine 2, 15
- ion beam dynamic mixing 225

- Jönsson–Hogmark model 264f
- Joule heating 46

- Kaufman stability criterion 68
- Knudsen number 104, 108

- ladles 15, 275
- Langmuir probe 35
- Laplace operator 150

- laser anemometer 81
- laser Doppler anemometry (LDA) 83ff, 101, 128
- laser irradiance 218f, 221
- latent heat of evaporation 118
- latent heat of fusion 109
- latent heat of melting 142
- lattice deformation 171
- Laval nozzle 74, 76, 88, 236
- Lewis number 318
- life-cycle curve 8
- Lorentz force 43, 52, 57, 58, 69, 125
- low-loading condition 113, 119

- Mach number 144, 236
- magnetic pinch 57, 64
- manufacturing industry 2
- marker and cell method 142
- Marsh's relation 266
- mass loss by vaporization 113
- mass transfer coefficient 113
- Maxwell distribution 31, 36–38
- Maxwell equation 48, 121
- Menstruum process 200
- mercury pressure porosimetry 165f
- metal properties
 - coefficient of thermal expansion 14, 169f, 174, 201, 218, 229
 - creep 277
 - creep strength 13
 - ductility 13
 - fatigue strength 13
 - flexural strength 13
 - fracture toughness 14
 - heat conductivity 14
 - porosity 14
- microelectronics industry 2
- microwave 44
- mining toll 15
- modulus of elasticity 170, 174, 178, 216, 217, 224, 267
- momentum transfer 22, 100ff, 108
 - from particles to substrate 141
 - from plasma to particles 50, 132
 - modeling 127

- Nabarro–Herring creep 217
- Navier–Stokes equation 57, 106, 121, 125, 317
- Nelson–Riley extrapolation function 174
- Neumann–Schwartz equation 319

- Neumann–Schwartz parameter 140
 Newton's law 104, 144
 Newton momentum equation 175
 nonlinearity 124, 174
 Nusselt number 108, 114, 125, 318
- Ohm's law 44, 48
 Ollard–Sharivker test 253
 Orowan–Petch relation 271
 orthopedic prostheses 15
 osmotic filtering 15
 osteogenesis
 – bonding osteogenesis 224
 – contact osteogenesis 224
 – distance osteogenesis 224
 oxygen sensor 82
- particle–substrate interactions 137ff
 particle diagnostics 128
 – particle emission 80
 – particle emissivity 108
 – particle flux 133
 – particle inertia 101
 – particle number density 128, 132f, 138, 141
 – particle number flux 78
 – particle temperature 104, 108, 109
 – particle temperature distribution 78
 – particle velocity 88, 101, 102, 106, 147, 149
 – particle velocity distribution 78, 130
 – plasma jet residence time 108f
 – residence time of the particles 231
 – temperature 128, 131, 132
 – velocity 128ff
 – wipe test 147, 154
- particle erosion 183
 particle impact 137, 142, 143, 147
 – catastrophic fragmentation 149
 – contact face perimeter 146
 – degree of flattening 155
 – elastic pressure 145
 – flattening ratio 141, 142, 248
 – hot spots 148
 – impact angle 142, 276
 – impact velocity 141
 – Mexican hat shape 138, 140
 – pancake shape 138
 – particle deformation 139
 – particle splats 137
 – rarefaction wave 147f
 – shock front 145, 146, 148
 – shock heating 147
- shock pressure 141, 146, 147
 – shock wave 137, 144, 147, 164
 – stress wave 144
 – thermal pressure 145, 146
 Péclet number 143, 318
 photon correlator 84
 pin-on-disc apparatus 268
 piston 15, 210
 Pitot tube 81f
 plasma–particle interactions 1, 91ff
 plasma 77, 226
 – characteristic plasma parameter 48
 – charge carrier 27, 41, 44, 46, 50
 – charge distribution 27
 – classification 31, 33, 35
 – cold plasmas 31, 35
 – d.c. plasmas 50
 – Debye screening length 35
 – definition 27, 30
 – electrical field strength 28, 52
 – electric plasma 34
 – electromagnetic plasma 34
 – electron density 31, 33–36
 – electron temperature 32, 33, 35, 40, 44, 48
 – equilibrium compositions 38
 – equilibrium conditions 48
 – equilibrium distribution 39
 – equilibrium plasma 35, 38, 40
 – heavy particle temperature 32, 35, 48
 – high density plasma 35
 – high frequency oscillation 28
 – isothermal plasma 38
 – local thermal equilibrium 50, 125
 – local thermodynamic equilibrium 32, 77
 – low density plasmas 32
 – magnetic field 35
 – magnetic field strength 32, 35, 125
 – magnetic plasma 34
 – medium density plasmas 32, 34
 – modeling of the plasma spray process 1
 – neutrality 27, 28
 – nonequilibrium plasma 35, 40
 – nonisothermal plasma 44
 – plasma energy 37, 121, 227
 – plasma enthalpy 38, 155, 184
 – plasma state 27, 34, 38
 – plasma temperature 32
 – R.F. plasmas 50
 – scalar plasma 35
 – self-confinement 57

- solid state plasma 35
- subnormal discharge 46
- temperature 35
- tensorial plasma 34, 35
- thermal plasma 32, 35, 48
- three-fluid plasma 35
- two-fluid plasma 35
- Vlasov plasma 32
- plasma arc 17
 - plasma arc properties
 - AJD mode 55
 - anode fall 46, 60
 - anode jet 52, 54, 55
 - anode region 55, 56
 - arc cathode 46
 - arc column 50, 52
 - arc current 82
 - arc discharge 46, 50
 - cathode fall 46, 50
 - cathode jet 52, 54, 55
 - characteristic 68
 - CJD mode 55
 - current density 50, 55
 - electron current 50
 - modeling of arc column 48
 - plasma column 42, 43, 55, 72
 - positive column 46, 50
 - positive-ion current 50
 - potential distribution 46, 47
 - space charge 46, 47, 50, 51
 - structure of the arc column 50
 - thermal boundary 46
 - wall-stabilized 50
 - plasma arc stabilization 68ff
 - convection-stabilized arc 68, 69
 - electrode-stabilized arc 69
 - gas-sheath stabilized plasma 69
 - gas-stabilized arc 63, 68
 - magnetically-stabilized jet 70
 - by thermal pinch 64
 - vortex stabilized arc 69
 - wall stabilized arc 68
 - water-stabilized arc 63
 - plasma chemical synthesis 37
 - plasma diagnostics 77ff
 - enthalpy measurement 77
 - fringe mode measurement 84
 - multiwavelength pyrometry 128
 - spectroscopic measurement of plasma temperature 80
 - spectroscopic methods 77
 - temperature measurement 77, 78
 - two-color pyrometry 132
 - two-wavelengths pyrometry 80
 - velocity measurement 77, 78, 81–83
- plasma etching 35
- plasma gas
 - air 64
 - argon 19, 38, 39, 55, 64, 77, 82, 109, 110, 114, 116, 207, 296
 - argon/hydrogen 128, 155, 296
 - collision ionization 38, 43, 44
 - dependent discharge 45
 - discharge characteristic 45
 - dissociation 38
 - drift velocity 44, 50
 - energy content 40
 - flow rates 82
 - gas ionization 38
 - gas velocity 101
 - heat conduction 52
 - helium 38, 130, 192
 - hydrogen 19, 55, 109, 110, 114, 116, 192, 207
 - independent discharge 45
 - ionization 38, 40, 41, 55
 - ionization energy 40, 45
 - ionization frequency 44
 - nitrogen 19, 38, 39, 55, 77, 109–111, 114, 116
 - oxygen 79
 - photoionization 38
 - Saha–Eggert equation 40
 - specific heat 41
 - thermal conductivity 117
 - viscosity 103
 - volume ionization 45
- plasma generation 38ff
 - abnormal glow discharge 46
 - a.c. discharge mode 44
 - adiabatic compression 43
 - arc cathode 46
 - ballistic compressor 42, 43
 - d.c. discharge mode 44
 - dependent discharge 44
 - discharge current 45
 - electron beam plasma generator 43
 - gas discharges 44
 - glow cathode 45, 46
 - glow discharge 45, 46
 - impulse mode 44
 - independent discharge 44

- laser radiation 44
- magnetic compression 57
- magnetic plasma confinement 41
- MHD generator 41
- pinch 52
- Θ -pinch apparatus 42, 43
- z-pinch apparatus 42, 43, 57, 58, 125
- plasma focus 42, 43
- plasma furnace 40, 42
- Q engine 41, 42
- quiet plasma 41
- shock tube 42, 43
- shock wave 43
- plasma jet 17, 21, 43, 52, 57, 70ff, 79, 81–83, 86, 91, 94, 101, 106, 119, 124, 125, 132, 139, 149
- eddies 74, 75, 77, 91, 125, 134, 208
- electrical potential field 22, 100
- enthalpy distribution 70, 74
- heat content 19
- jet core 80, 84
- laminar 75
- modeling 101
- momentum transfer 101
- plasma core 74
- quasi-laminar jets 74
- quasi-laminar plasma 77
- ring vortex 73
- temperature distribution 71, 73, 80
- turbulence 101, 104, 125, 133, 134
- turbulent plasma 60, 70, 72, 74, 75, 84, 86, 88, 91, 103, 208
- velocity distribution 71, 72
- plasma parameters 28ff
 - characteristic distance 31, 35, 36
 - collision cross-section 30, 31
 - collision frequency 28, 31, 36
 - collision path length 30, 31, 36 see also mean free path length
 - Coulomb logarithm 30
 - cyclotron path 32
 - Debye screening length 28–31, 36
 - Debye sphere 29, 30
 - elastic collision 30
 - electron temperature 31
 - heavy particle temperature 31
 - inelastic collision 30
 - Landau length 28, 29 see also critical distance
 - Langmuir oscillation 43
 - Langmuir plasma frequency 28, 31, 36
- see also collision length
- Larmor radius 32, 36
- Larmor rotation 32
- macroscopic plasma parameters 70
- Maxwell–Boltzmann distribution 30
- mean free collision paths 32
- mean free path length 28, 30, 108
- microscopic parameters 28
- particle velocity 143
- particle viscosity 184
- plasma condition 32, 34
- plasma density 81, 82
- plasma parameter 29, 32
- plasma pressure 30, 57, 101, 317
- plasma temperature 77, 80, 82, 104, 108, 114, 118, 119, 122, 128, 184
- plasma velocity 70, 82, 84, 86, 101, 102, 113, 125, 126, 128, 231, 317
- plasma viscosity 81, 113, 125, 317
- relaxation time 31
- temperature gradient 70, 81, 126, 129
- plasma spheroidizing 37, 94
- plasma spray parameters 20, 21, 23
 - design factors 97
 - argon gas pressure 324
 - chamber pressure 227, 296ff
 - feed rate 128
 - particle-size distribution 97
 - plasma arc current 324
 - plasma power 128, 155, 227, 229, 296ff
 - powder feed rate 227, 296ff, 324
 - powder gas pressure 324
 - spray distance 324
 - stand-off distance 128, 155, 227, 229, 296ff
 - substrate temperature 227, 229
 - traverse speed 296ff
 - divergence 77
 - gas pressure 19
 - grain size 19
 - injection angle 19
 - powder feed rate 19
 - powder gas pressure 19
 - power input 19
 - spray atmosphere 19
 - spray distance 19
 - spray divergence 19
 - stand-off distance 77
 - traverse rate 19

- plasma spray particles
 - injection of powders 91
- plasma spray powder
 - powder injection 64, 70, 74, 92
- plasma surface modification 35
- plasma/thermal spray powder
 - injection 133, 186
 - injection probe 133
 - powder characteristics 95, 96, 246
 - powder microstructure 95
 - powder morphology 95
 - size distribution 94, 97, 99, 138, 247
- plasmatron 8, 17–19, 43, 48, 50, 55ff, 62, 67–69, 72, 76, 77, 84, 91, 99, 119, 127, 137, 139, 186, 190, 194, 231, 287, 304, 313
 - arc discharge generator 57, 59
 - arc-welding configuration 61
 - electrode plasma (EP) 59
 - electrodeless plasma (ICP) 59
 - electrodeless plasmatron 65
 - inductively-coupled plasma (ICP) devices 63, 67
 - inductively-coupled plasmatron 66, 122, 123
 - inductively-coupled torch 64
 - nontransferred arc 63
 - nontransferred electrode plasmatrons 59, 60
 - nontransferred plasma 59, 62
 - transferred arc 61–63
 - transferred electrode plasmatrons 61
 - transferred plasma 59
- plasmatron electrode 66
- plungers 183, 202
- point counting 165
- Poisson's law 50
- Poisson ratio 170, 171, 174, 177, 178
- post-spraying treatment
 - hot isostatic pressing 14, 165, 218, 229
 - infiltration 14, 165, 218
 - laser densification 14
 - laser-glazing 202, 218
 - laser surface densification 165
 - laser surface remelting 218
 - post-spray grinding and polishing 202
 - pulsed laser sealing 223
 - reactive laser treatment 223
 - sealing 218
- Prandtl number 108, 125, 318
- printing rolls 15
- PSI model 121
- pump plungers 15
- PVD sputter targets 15
- quality control 243ff, 248, 313
 - coating quality 24
 - continuous improvement 243, 245
 - management style 243, 245
 - plasma spray powders 98
 - qualification procedure 245f
 - quality coating 244, 248
 - quality function deployment (QFD) 10, 97, 244
 - quality philosophie 243ff
 - quality tools 243f
 - statistical experimental design 212
 - statistical process control (SPC) 10, 97, 122, 244, 311
 - statistical quality assurance (SQA) 244
 - statistical quality control (SQC) 244
 - Taguchi analysis 122
 - total quality management 94, 225, 243ff
- Raman shift 231
- random walk influence 134
- Rankine–Hugoniot equation 144f
- rapid solidification 288
- rapid solidification technology 141, 167, 223
- Rayleigh number 125, 318
- reactive plasma processing 66
- reciprocating pumps 183, 202
- resorption resistance 226, 232
- Reynolds number 64, 81, 101, 103, 104, 114, 318
- Richardson–Dushman equation 51
- Riemann–Hugoniot catastrophe 125
- Ryshkevich–Duckworth equation 271
- saturation current 44
- Schmidt number 114, 318
- Schottky correction 51
- Schumann–Runge bands 79
- screening test 277
- self-sharpening 203f
- service life prediction 279
- Sharivker/Ollard test 249f
- Sherwood number 114
- shot peening 175
- shrouds 15
- solid oxide fuel cells (SOFC) 233ff
- solid-particle erosion (SPE) 187, 198, 271, 274

- solidification time 137, 140, 141, 147, 149, 152
- SPE resistance 196
- specific heat flux 114, 117
- spray powder production
 - agglomeration 94, 100, 196
 - arc-fuse/crush powders 97, 99
 - arc-fuse/spray-dry 97f
 - atomization 94, 97
 - chemical cladding 100
 - compositing 100
 - fluidized bed sintering 94
 - fusing/melting 94
 - fusion and crushing 97
 - gas-atomized particles 97, 100
 - hollow-spherical-powder (HOSP) 97, 99
 - hydrogen pressure-reducing powder coating (HYPREPOC) 100
 - spray drying 94
 - water-atomized particles 97, 99, 100
- spraying parameters 10
- stagnation enthalpy 81
- statistical design of experiments (SDE) 246
- steele bridges 15
- Stefan–Boltzmann coefficient 126
- Stefan–Boltzmann constant 108
- Stefan–Kutateladze group 142f
- Stefan number 125, 318
- Stokes equation 104
- strain gauges 170
- strain to fracture (STF) 267
- stress corrosion cracking 196
- substrate
 - AISI 304 199
 - AISI 410 199
 - AISI 422 198
 - AISI 5150 steel 186
 - aluminum 6, 167, 172, 224, 225, 253
 - 6061 aluminum 298f
 - austenitic steel 177, 294, 309
 - austenitic superalloy 209
 - bioactive glasses 224
 - carbon 224
 - carbon fiber composites 181
 - carbon steel 303
 - cast iron 6
 - ceramics 8
 - CK 45 287
 - Co–Cr alloys 224
 - copper 6, 164, 206, 258ff
 - Cr₇C₃ 263
 - ferritic steel 177
 - graphite 181
 - Hastelloy X 199, 207
 - hot-rolled sheet stell (A 569) 202
 - Inconel 617 213ff
 - Inconel 800 199, 207
 - low-carbon steel 140, 152f, 299
 - MCrAlY 209
 - metal foil 255
 - mild steel 187, 253, 271, 293, 294, 296–298, 308
 - Ni-based superalloy 217
 - nickel 6
 - PWA 1460 206
 - SiC 263
 - stainless 6
 - 304 stainless steel 177, 223, 224
 - steel 6, 8, 139, 151, 152, 167, 168, 174, 181, 183, 208, 293
 - St 37 steel 172f
 - substrate heating 19
 - superalloys 6, 206
 - surface roughness 19
 - tantalum 224
 - Ti6Al4V 226, 229
 - TiO₂ 263
 - titanium 224–226
 - vanadium alloys 8
 - VC 263
 - WC/Co 203f
 - zirconia 224
- superconductivity 233
- superheaters 15
- surface-tension gradient 220f
- Taber apparatus 268
- thermal conductivity 152, 161, 216, 220, 320ff
 - contact thermal conductivity 151, 320ff
 - mean boundary layer thermal conductivity 113
 - of the particles 109
 - of plasma gas 109
 - substrate with higher thermal conductivity 142
- thermal diffusion (heat conduction) equations 152
- thermal diffusivity 112, 150, 220, 319ff
- thermal pinch 55
- thermal spray powder 94

- thermal spraying methods 1, 2, 8ff, 17ff, 21ff
 - air plasma spraying (APS) 17, 19, 21–23, 94, 183, 187, 192, 196, 199, 205, 226, 248, 297
 - arc spraying 22
 - arc wire-spraying 127
 - controlled atmosphere plasma spraying 17
 - D-Gun 21, 22, 143, 144, 183, 196, 198
 - detonation gun techniques 94
 - electric arc spraying 93
 - electric arc wire-spraying 19, 22
 - flame spraying 8, 22, 93, 183, 205
 - high power plasma spraying 17
 - hypervelocity oxyfuel gun (HVOF) 21, 22, 94, 143, 144, 168, 183, 192, 205, 226, 231
 - inductive plasma spraying (IPS) 21, 22
 - inductively-coupled RF plasma 130
 - inert gas plasma spraying (IGPS) 17, 23
 - Jet Kote system 21, 22
 - laser spraying 19
 - low pressure laser spraying (LPLS) 22
 - low pressure plasma spraying (LPPS) 17, 19, 104, 132, 165, 183, 206, 248
 - oxyacetylene torch 22
 - plasma transferred arc (PTA) 297
 - PTA surfacing 308
 - radio-frequency spraying (RF) 21
 - reactive plasma spraying 183, 192ff
 - RF ICP 231, 233, 235
 - RF-plasma spraying 22
 - SPS 17
 - underwater plasma spraying (UPS) 19, 23, 183
 - vacuum plasma spraying (VPS) 17, 21–23, 94, 156, 183, 196, 199, 205, 226
- thermionic work function 53
- thermophoresis 129
- thermophoretic effect 101
- time-resolved infrared radiometry 259
- Townsend coefficient 44, 45
- Townsend discharge 45, 46
- Townsend ignition condition 45
- tribomaterials 269f
- tundishes 15, 275
- turbine blade 274
- turbine vanes 15
- ultimate tensile strength (UTS) 206
- ultrafiltration 15
- valves 15, 210, 223, 274
- Washburn equation 166
- water electrolyzers 236
- wear mechanisms
 - abrasive wear 269ff, 274
 - adhesive wear 269f
 - erosive wear 271
 - flank wear 287
 - long-term fatigue wear 271, 273
- Weibull modulus 178, 268
- welding process 127, 137
- Wheatstone bridge 170
- X-ray small angle scattering 165
- Young's modulus 171, 175, 177, 198, 211, 249

Plasma-Spray Coating

by Robert B. Heimann

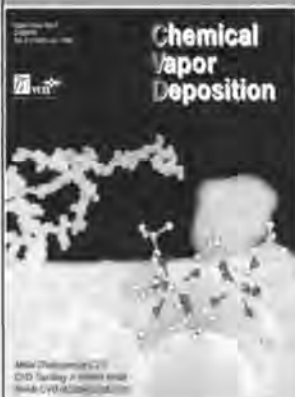
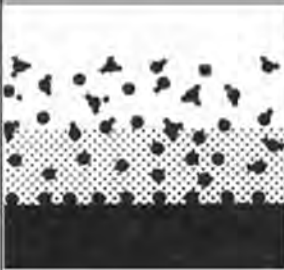
Copyright © VCH Verlagsgesellschaft mbH, 1996

Rees, W.S., Jr. (ed.)

CVD of Nonmetals

1996. 400 pages with 100 figures and 60 tables. Hardcover.
ISBN 3-527-29295-0

Written by leading experts in the field, this handbook offers an up-to-date, critical survey of this burgeoning field of research. Technological issues as well as new scientific results are discussed and the viability of the method, both technically and economically, is compared with other deposition techniques available.



Get the hottest peer
review research results on
chemical vapor deposition!

Jones, A.C./O'Brien, P.

CVD of Compound Semiconductors

Precursor Synthesis, Development and Applications

1996. 450 pages. Hardcover. ISBN 3-527-29294-2

Chemical growth methods of electronic materials are the keystone of microelectronic device processing. This book details the chemistry of the precursors used in the deposition of various materials and makes the science and technology of deposition accessible to the materials scientist.

Chemical Vapor Deposition (CVD)

ISSN 0948-1907

6 issues per year

CVD is published every two months as a special section of the world's leading material science journal **Advanced Materials**. The deposition of thin films of metal, ceramics, and semiconductors using CVD, their characterization, related vacuum technology and equipment, and related aspects of surface science are core areas covered in this journal.

Our standard setting stringent referee system on all papers submitted guarantee high quality papers from renowned experts around the globe.

Don't miss out on the latest results,
developments and trends in your field.

Order your free sample copy!

